Astron. Astrophys. 347, 375–390 (1999)

ASTRONOMY AND ASTROPHYSICS

High resolution emission spectroscopy of the A $^1\Pi$ – X $^1\Sigma^+$ fourth positive band system of CO excited by electron impact

Luther W. Beegle, Joseph M. Ajello, Geoffrey K. James, Dariusz Dziczek, and Marcos Alvarez

Jet Propulsion Laboratory, California Institute of Technology, Mail Stop 183-601 Pasadena, CA 91109, USA

Received 22 October 1998 / Accepted 25 March 1999

Abstract. We report electron-impact-induced medium resolution fluorescence spectra of CO [310 mÅ and 366 mÅ full width at half maximum (FWHM)] at 100 eV over the spectral region from 1300 to 2050 Å. Features in the far ultraviolet (FUV) emission spectra correspond to the Fourth Positive band system of CO (A $^1\Pi$ – X $^1\Sigma^+$), together with atomic multiplets from C and O and their ions. The absolute electronic transition moment as a function of internuclear distance was determined from relative band intensities scaled to oscillator strength measurements. A model of the vibronic structure of the band system was developed using the laboratory measurement of the electronic transition moment. In addition, we have obtained high resolution spectra ($\approx$ 34 mÅ FWHM) of the CO (A-X) (5,1) band at 1435 Å and the (3,0) band at 1447 Å and accurately modeled the rotational line structure. The excitation function of the (0,1) band at 1597 Å was measured in the electron impact energy range from threshold to 750 eV and normalized at 100 eV using the relative flow technique with the standard NI (1200 Å) cross section from dissociative excitation of N_2. The CO (A-X) band system emission cross section was established from a measurement of the relative band intensities of CO at 100 eV. The total Fourth Positive band system cascade cross section, arising from (B $\rightarrow$ A) and (C $\rightarrow$ A) transitions, is $\sim$ 6% of the emission cross section at 100 eV. The high resolution line profile of the 1152 Å atomic O multiplet ($^1D^0$- ^1D) resulting from dissociative excitation of CO was measured at $\sim$ 22 mÅ FWHM. Kinetic energy distributions of the atomic O fragments at 30 eV and 100 eV impact energies were obtained from an analysis of the deconvolved true line profiles.

Key words: molecular data – ISM: molecules – ultraviolet: ISM

1. Introduction

The CO Fourth Positive band system (A $^1\Pi$ – X $^1\Sigma^+$) is ubiquitously observed in astronomy, appearing in UV spectra from the sun, the planets and the interstellar medium (ISM). The CO (A-X) system plays an important role in understanding the conditions and chemistry in the ISM, where it has been observed in absorption by the Hubble Space Telescope (HST) toward the β-Pictoris circumstellar disk (Jolly et al. 1998) and ζ Ophiuchi (Sheffer et al. 1992; Lyu et al. 1994; Lambert et al. 1994). As the most abundant interstellar molecule after H_2 (van Dishoeck, Black 1988) the accurate analysis of CO from its UV absorption spectrum plays a significant role in understanding the photochemistry of the ISM. The (v'' =0) absorption bands vary in intensity over several orders of magnitude such that accurate band oscillator strengths over the entire range of observed vibrational levels from v' =0 to 12 in the ISM are needed. This large range of variation normally allows the measurement of unsaturated absorption for at least one v' value along a particular line of sight. Marked progress has been made in recent years concerning the oscillator strengths. The latest measurements of f-values summarized by Eidelsberg et al. 1998 are in good agreement for $v' < 8$, typically to within $\sim$ 5%. For higher v', the oscillator strength values measured recently by Jolly et al. 1997, Stark et al. 1998 and Eidelsberg et al. 1998 are also in agreement, typically to within 20%. The data of Federman et al. 1997 for intermediate v' are systematically lower than those of Chan et al. 1993 and Jolly et al. 1997, but within stated uncertainties.

The CO Fourth Positive band system emission spectrum has been observed in the airglow spectrum of Mars and Venus in the 1200–1800 Å region. The (A-X) band system is excited in the thermosphere by the impact of photoelectrons and the effect of solar UV photons on both CO and CO_2 (Barth et al. 1992; Fox 1992). The v' =14 level of the CO (A-X) system is of particular interest on Venus because the transition from v'' = 0 is resonant at a wavelength of 1215.5 Å, which lies within the width of the very strong solar Lyman-α line. Accurate modeling of the processes producing the airglow emission spectra from either of these planets will only be as accurate as the set of CO (A-X) emission cross sections for CO and CO_2 from electron and photon impact. The CO (A-X) fluorescence spectrum from the sun has also been observed (Bartoe et al. 1978; Jordan et al. 1979). The v' =0, v'' progression is produced in the sun by fluorescence from the C IV transition-zone lines at 1548 Å and 1551 Å which excite the (0,0) band from high J''.

Accurate values of emission cross sections and oscillator strengths are needed for analysis of the CO (A-X) absorption and emission spectra from astrophysical sources. The recent

Send offprint requests to: Joseph M. Ajello

history of the experimental determination of band oscillator strengths for the CO Fourth Positive system is summarized in a review paper by Morton & Noreau 1994, and updated for high v' by Federman et al. 1997, Jolly et al. 1997, Stark et al. 1998 and Eidelsberg et al. 1998. The latter authors also present recommended oscillator strength values for v' = 0 to 23. Ab initio calculations of the CO (A-X) oscillator strengths have been made by Kirby & Cooper 1989, Chantranupong et al. 1992 and Spielfiedel et al. 1998. Three experimental techniques have been used to measure oscillator strengths: band averaged lifetime measurements (Field et al. 1983), electron energy loss spectroscopy (Chan et al. 1993; Zhong et al. 1997) and optical absorption spectroscopy (Eidelsberg et al. 1998; Smith et al. 1994; Federman et al. 1997; Jolly et al. 1997; Stark et al. 1998). Variations in the measured oscillator strengths are now at the 5% level for low v', and within $\sim$20% for high v'. These discrepancies are considerably smaller than for the higher lying states (B, C and E) where measurements differ by factors of two (Ciocca et al. 1997a; Morton & Noreau 1994). The most recent experimental work on oscillator strengths by Eidelsberg et al. 1998 for v' = 11 to 23, by Stark et al. 1998 for v' = 13 to 21, by Jolly et al. 1997 for v' = 9 to 17, by Federman et al. 1997 for v' = 7 to 11, and by Smith et al. 1994 for v' = 11 to 14, have resolved the main discrepancies in oscillator strength values described by Morton & Noreau 1994. Differences in the reported oscillator strengths of Eidelsberg et al. 1998, Stark et al. 1998 and Jolly et al. 1997 for $v' > 12$ tend to be $<$ 20%, with the latter two authors typically agreeing to better than 10%. Federman et al. 1997 point out that their results agree with those of Chan et al. 1993 to within stated experimental uncertainties, though the Federman et al. 1997 values are systematically 15–20% lower than the Chan et al. 1993 data.

Our main goals in this work are: 1) to measure the emission cross section from threshold (at 8 eV) to 750 eV for the CO Fourth Positive band system (A $^1\Pi$ -X $^1\Sigma^+$) consisting of about 100 vibronic features and 2) to determine the variation in the electronic transition moment over the range of internuclear distances from 1.05 to 1.4 Å. To achieve both goals we measure the intensity of every feature in the wavelength range from 1300 to 2050 Å at medium resolution under optically thin conditions at 100 eV electron impact energy. We ratio each measured intensity to the intensity of the CO (0,1) band at 1597 Å. The electron impact excitation function of the CO (0,1) band is measured from threshold to 750 eV. We determine the absolute cross section of the CO (0,1) band (and hence the cross sections for all the other features) by utilizing the relative flow technique at 100 eV with a standard gas (Ciocca et al. 1997a).

It is timely to perform the first excitation function measurements of the CO (A-X) system in 30 years (Aarts & de Heer 1970; Mumma et al. 1971; Ajello 1971a) for various reasons: 1) optical calibration benchmark electron impact cross sections in the UV (such as H_2 Lyman-α, the ultimate reference for the NI (1200 Å) standard cross section (James et al. 1990)) have decreased by almost a factor of 2 from the cross section work of Mumma et al. 1971 (see Ajello et al. 1988), 2) the accepted f-value calibration standard for v' =0 of Morton & Noreau 1994 is $\sim$11% lower than that used in the cross section works of Aarts & de Heer 1970 and Ajello 1971a, and 3) cascade estimates from the early work (Aarts & de Heer 1970) differ by a factor of $\sim$5 from the values found in Letzelter et al. 1987 for the B $^1\Sigma^+$ – A $^1\Pi$ and C $^1\Sigma^+$ –A $^1\Pi$ cascade transitions.

The excitation cross section for A $^1\Pi$ v' =0, $\sigma_0^{excitation}$, can be calculated from the experimental value of the emission cross section from A $^1\Pi$ v' =0, $\sigma_0^{emission}$, and the calculated cross section for cascade to A $^1\Pi$ v' =0 from the higher B and C states, $\sigma_0^{cascade}$, (see Sect. 6), using the following relation:

$$\sigma_0^{excitation} = \sigma_0^{emission} - \sigma_0^{cascade} \quad (1)$$

The excitation function of the A $^1\Pi$ – X $^1\Sigma^+$ (0,1) band from threshold to 750 eV, corrected for cascade from the v' = 0 levels of the higher-lying B and C states and normalized at 100 eV, is presented. The original published cross section values presented 30 years ago by Aarts & de Heer 1970, Mumma et al. 1971 and Ajello 1971a, were in agreement to within $\sim$10%. However, correcting their data for the calibration changes in 1) and 2) described above now yields 100 eV emission cross section values that are significantly different. The original agreement is found to be fortuitous.

Utilizing the spectral scans from 1300 to 2050 Å we have determined the electronic transition moment as a function of internuclear separation and have found it to be in excellent agreement with (among others) Chan et al. 1993, Kirby & Cooper 1989 and Spielfiedel et al. 1998. The only previous determination of the electronic transition moment using electron impact induced fluorescence by Mumma et al. 1971 was over a more limited range of internuclear distances (1.05 to 1.35 Å). Morton & Noreau 1994 have indicated substantial changes in the Mumma et al. 1971 electronic transition moment. The transition probabilities for the band system calculated by Mumma et al. 1971 need to be recalculated based on the combination of the electronic transition moment from this work and the works of De Leon 1988, De Leon 1989 over a range of distances (1.0 to 1.8 Å).

We summarize the presentation of the paper as follows: Firstly, the experimental apparatus is described. We also outline the relative flow technique for determination of the CO (0,1) emission cross section at 100 eV. The medium resolution spectrum, calibrated for wavelength sensitivity, is shown and compared to models. This spectrum is used as a basis for determining the total cross section at 100 eV, the variation in the electronic transition moment and the transition probability array for the band system. We then show the high resolution spectra of two CO (A-X) bands and one atomic line with fine structure models. Finally, the measurement of the CO (A-X) (0,1) excitation function from threshold to 750 eV is described. We utilize previous results from this laboratory to calculate the cascade cross section for the (B-A) and (C-A) transitions. The emission cross section is subsequently described as a sum of excitation and cascade cross sections in tabular and pictorial form. A discussion section follows.

2. Experimental apparatus and procedure

The experimental apparatus has been described in detail elsewhere (Liu et al. 1995; Ajello et al. 1996). The apparatus consists of an electron-impact collision chamber in tandem with a high-resolution Acton 3.0-meter UV spectrometer. The FUV emission spectra of CO were measured by crossing a magnetically collimated beam of electrons with a beam of CO gas formed by a capillary array at 90°. A Faraday cup, designed to minimize backscattered and secondary electrons, was used to monitor the electron current. The impact energy of the electron beam was fixed at either 20 or 100 eV during spectral scans. Emitted photons, corresponding to radiative decay from the collisionally excited states of CO, were observed at 90° to both the electron beam and molecular beam by the UV spectrometer. The spectrometer was equipped with a CsI-coated channeltron detector or an F-type photomultiplier tube (PMT) with a bi-alkali CsTe photocathode. The collision region was 11.05 cm from the entrance slit to the spectrometer. Scanning in wavelength was achieved by means of an indexed stepper motor. Step sizes were programmable in Å and could be maintained at 1/4 to 1/5 the value of the instrumental resolution.

The CO (A-X) spectra were calibrated using instrument sensitivity curves generated from electron impact studies of the fluorescence spectra of the calibration gases N_2 and H_2. With H_2 as the calibration gas, the model and laboratory FUV spectra from 1100–1700 Å at 4 Å resolution (FWHM) for the H_2 Rydberg band systems at 100 eV were divided into 29 wavelength regions, as identified by Liu et al. 1995. The ratio of the area under the observed features of the laboratory spectrum to the area under the features of the model spectrum defines the spectrometer-detector sensitivity. In a similar manner (Ajello et al. 1988), with N_2 as the calibrating gas, the low resolution model spectra from 1200–2200 Å for the N_2 Lyman-Birge- Hopfield band system and the NI atomic multiplets from dissociative excitation at 30 eV and 100 eV were compared to low resolution experimental spectra. The calibrated sensitivities for both the channeltron detector and the PMT, in the region where the sensitivities allow such comparisons, were identical for the two calibration gases. A typical sensitivity curve for the 3m spectrometer with a CsI-coated channeltron is shown in Liu et al. 1995.

For the high resolution FUV spectra of the (5,1) 1435 Å and (3,0) 1447 Å bands a resolving power of $\lambda/\Delta\lambda \approx 40\,000$ was achieved by operating the spectrometer in second order with both entrance and exit slit widths set at 20 μm. The slit function was triangular with a resolution of 34 mÅ FWHM.

Medium resolution spectra in the range 1300–2050 Å were obtained in first order with both slit widths set at 100 μm, corresponding to a FWHM of $\sim$300 mÅ. Spectra were measured at both low and high capillary head pressures. The low head pressure produced an operating background pressure of 1×10^{-5} torr. This resulted in an optical depth for $J' = 7$ of less than 0.1, ensuring that the strengths of the (v', 0) features were not reduced as a result of self-absorption. The high head pressure produced an operating background pressure of 2×10^{-4} torr and the spectra were optically thick in the strongest (v',0) resonance transitions. In addition, the rotational temperature was cooled from 300 K laboratory temperature to 175 K as a result of adiabatic expansion at the tip of the effusive capillary. The relative strengths of the (v',v'') transitions for $v'' \neq 0$ were nearly identical at the two pressures. Using higher pressure facilitated the detection of some of the weaker bands. The spectra at 1×10^{-5} torr were optically thin with a 300 K rotational temperature. The intensities of the v' to $v'' = 0$ resonance bands measured at the higher head pressure were not used in the 100 eV band system cross section measurement or R_e determination due to effects of self-absorption.

In order to perform the relative flow calibration at 100 eV for the unknown CO (0,1) (1597 Å) cross section a gas mixture of 20% N_2 and 80% CO was introduced into the electron collision chamber at very low head pressures, typically 100–300 mTorr ($1–5\times10^{-6}$ Torr background pressure). Relative intensities of the standard NI atomic feature at 1200 Å due to dissociative excitation of N_2 and the unknown CO (0,1) band at 1597 Å were compared at 100 eV under the same single-scattering optically thin conditions (electron gun current, pressure etc.). After correcting for the sensitivity of the detector, and utilizing the initial 4:1 ratio in number of molecules, the ratio of the cross section of the NI 1200 Å feature to the CO (0,1) band at 1597 Å was determined to be 3.57. Using the known 100 eV cross section of the dissociative excitation multiplet of N_2 at 1200 Å, 4.0×10^{-18} cm^2 (James et al. 1990), yields an emission cross section value for the CO (0,1) band at 1597 Å of 1.12×10^{-18} cm^2 at 100 eV. This absolute cross section at 100 eV allows direct calculation of the remainder of the 100 or so vibronic cross sections from the calibrated intensities observed in the spectra from 1300 to 2050 Å. To verify the accuracy of this technique, the intensities of the 1200 Å NI and 1492 Å NI/N_2 lines were compared to each other. The calculated cross section of the 1492 Å line was 1.26 x10^{-18} cm^2, which is in experimental agreement with the known value of 1.45 x10^{-18} cm^2 (Ajello & Shemansky 1985). The 20 eV CO (A-X) (0,1) emission cross section was derived from the relative intensity of the 1597 Å feature at 20 eV and 100 eV, yielding a value of $\sim 2.2\times10^{-18}$ cm^2. Ajello 1971a has previously shown the CO (A-X) excitation function to peak near 20 eV. A similar result was obtained in this work.

3. Medium resolution spectra of the CO $A^1\Pi$ - $X\,^1\Sigma$ band system

The medium resolution electron impact spectrum of CO in the FUV region obtained with the PMT at a pressure of 2×10^{-4} torr and at a resolution of 310 mÅ (FWHM), together with a model fit (described later) at 100 eV are shown in Fig. 1. The optically thin 100 eV spectrum (366 mÅ FWHM) measured with the CsI-coated channeltron at 1×10^{-5} torr, together with a model fit is shown in Fig. 2. The channeltron spectrum shows excellent agreement between the observation and the model, while the PMT spectrum has a very good agreement except for the $v'' = 0$ resonance bands due to the high head pressure, described above.

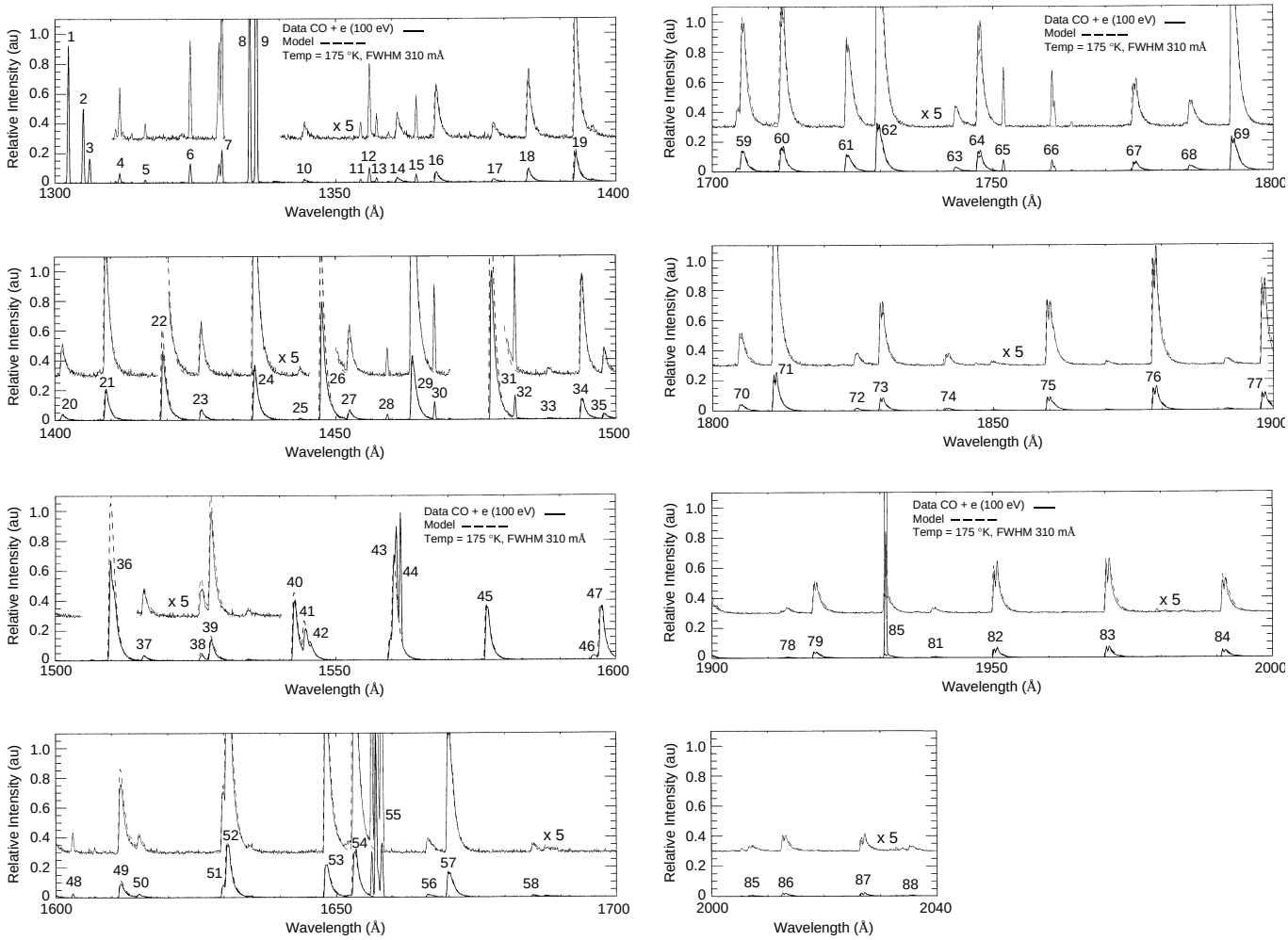

Fig. 1. Spectra of the CO (A-X) Fourth Positive band system between 1300 and 2050 Å (solid line) obtained with a photomultiplier tube at 100 eV electron impact energy and the corresponding model (dashed line).

The spectral wavelengths were calibrated with the atomic lines of C and O resulting from dissociative excitation. The spectral features and absolute emission and excitation cross sections are listed in Table 1. The root- sum-square uncertainty in the absolute emission cross sections given in this work was estimated to be 25% based on uncertainties in the N_2 reference cross section, the relative instrument sensitivity with wavelength and the signal statistics.

Identifications of the CO (A-X) features found in Table 1 were taken from the medium resolution model described in Sect. 5 by closely matching the observed wavelength for the peak signal (band head) with the close-lying calculated band origin. Some weak features found in Fig. 1 and Fig. 2 were identified from the model since they did not have a repeatable measured intensity.

Several of the Fourth Positive bands have multiple transitions that fall within the instrumental FWHM, resulting in blending. In order to obtain the cross sections of blended features we calculated the theoretical intensities of each of the features from the medium resolution model. The cross sections are the ratio of the relative intensities. In addition, the peak wavelengths of the blended features were taken to be the theoretical peak wavelengths.

The total experimental emission cross section of the CO (A-X) band system in Table 1 represents $\sim$98% of the total band system based on the generated model.

The value of 34.4×10^{-18} cm^2 listed at the end of Table 1 represents the sum of emission cross sections at 100 eV measured over the wavelength range from 1300–2050 Å. Several features with high v'' values longward of the cutoff at 2050 Å were not accounted for, and they contribute the majority of the missing 2%. Features with cross sections less than $\sim 4\times10^{-21}$ cm^2 ($\sim$1000 times lower than the cross section of the strongest feature) were too weak to be identified. The contribution of these unidentified weak features to the total emission cross section of the band system is insignificant. A 2% correction to the CO (A-X) band system would result in a total emission cross section of 3.51×10^{-17} cm^2 at 100 eV.

Table 1. Absolute cross section measurements of the A-X transition of CO produced by electron impact at 100 eV and 20 eV. Values in parentheses indicate theoretical values. Blended features are represented by a * in place of a feature number and the cross sections were separated utilizing theoretical intensities.The excitation cross sections were calculated by taking into account the calculated cascade cross sections from the higher B and C states for transitions up to $v' = 6$. Total experimental emission cross section at 100 eV = 34.4×10^{-18} cm^2

Feature No.	CO Transition v'	CO Transition v''	Atomic Identification	Peak Wavelength Å	Band Interval Start Å	Band Interval Stop Å	Cross section (x 10^{-18} cm^2) Emission 100 eV	Excitation 100 eV	Emission 20 eV
1			O I g^3P–$^3S_0$	1302.2	1301.4	1303.1			
2			O I g^3P–$^3S_0$	1304.9	1304.5	1305.4			
3			O I g^3P–$^3S_0$	1306.0	1305.5	1306.5			
4			C1 ^1D–$^1D^0$	1311.4	1310.4	1312.2			
5	12	2		(1316.0)	1315.5	1316.7	0.002		
6			CII ^2D–$^2D^0$	1323.9	1323.5	1324.6			
7			CI g^3P–$^3P^0$	1329.6	1328.6	1330.1			
8			CII g^2P^0 -^2D	1334.5	1333.9	1335.2			
	15	4		1334.6			0.001		
9	11	2		1335.4	1335.2	1337.1	0.006		
			CII g^2P^0 -^2D	1335.7					
10	7	0		1344.2	1343.8	1346.0	0.043		
11			CI ^1D–$^1P^0$	1354.3	1353.3	1354.7			
12			CI ^1D–$^1F^0$	1355.8	1355.3	1356.7			
13	10	2		1356.0	1355.3	1356.7	0.019		
14	8	1		1360.8	1360.5	1362.8	0.076		0.09
15			CI ^1D–$^1D^0$	1364.2	1363.7	1364.6			
16	6	0		1367.7	1367.3	1369.7	0.168	0.16	0.26
17	9	2		1377.9			0.054		0.06
18	7	1		1384.1	1383.8	1386.4	0.207		0.27
19	12	4		1392.1	1392.1	1396.6	0.003		
	5	0		1392.7			0.512	0.49	0.8
20	8	2		1401.1	1400.7	1403.6	0.105		0.16
21	6	1		1409.0	1408.3	1412.1	0.515	0.49	0.88
22	9	3		1418.7	1418.5	1424.1	0.028		0.04
	4	0		1419.1			1.522	1.44	2.18
23	7	2		1425.9	1425.4	1428.2	0.167		0.23
24	5	1		1435.4	1435.1	1439.8	0.932	0.89	1.26
25	8	3		1443.4	1443.1	1444.4	0.016		
26	3	0		1447.4	1446.8	1451.6	3.050	2.88	4.31
27	6	2		1452.3	1451.6	1455.2	0.173	0.17	0.24
28			CI ^1D–$^1P^0$	1459.0	1458.7	1459.5			
29			CI ^1D–$^1F^0$	1463.3	1462.7	1466.7			
30	4	1		1463.6	1462.7	1466.7	1.195	1.13	1.59
31	2	0		1477.6	1476.7	1483.2	4.094	3.83	6.37
32	10	5		1480.3	1476.7	1483.2	0.006		
33	8	4		(1487.7)	1487.4	1489.3	0.021		
34	3	1		1493.8	1493.2	1493.8	0.372	0.35	0.61
35	6	3		1497.7			0.080	0.08	0.15
36	1	0		1509.9	1509.0	1515.3	2.742	2.55	5.25
	4	2		1510.4			0.131	0.13	0.40
37	7	4		1515.7	1515.3	1515.7	0.083		
38	10	6		1525.7	1525.3	1527.8	0.001		
	2	1		1526.0			0.088	0.08	0.15
39	5	3		1527.7	1527.3	1530.7	0.372	0.35	0.65
40	3	2		1542.5	1542.0	1548.7	1.101	1.04	2.22
41	0	0		1544.4	1542.0	1548.7	0.551	0.51	1.09
42	6	4		1545.5	1542.0	1548.7	0.106	0.10	0.23
43	4	3		1559.7	1559.0	1566.2	0.471	0.45	0.84
44	1	1		1560.4	1559.0	1566.2	1.247	1.16	2.97
45	2	2		1576.9	1576.1	1581.3	1.056	0.99	1.92
46	6	5		1595.8	1595.3	1601.9	0.066	0.06	0.12

Table 1. (continued)

Feature No.	CO Transition v'	CO Transition v''	Atomic Identification	Peak Wavelength Å	Band Interval Start Å	Band Interval Stop Å	Cross section (x 10^{-18} cm^2) Emission 100 eV	Excitation 100 eV	Emission 20 eV
47	0	1		1597.3	1595.3	1601.9	1.120	1.03	2.28
48	9	7		1602.9	1602.3	1604.1	0.013		
49	4	4		1611.6	1610.9	1616.4	0.282	0.27	0.57
50	7	6		1614.8	1610.9	1616.4	0.064		
51	5	5		1629.8	1628.6	1635.9	0.276	0.26	0.44
52	2	3		1630.6	1628.6	1635.9	1.035	0.97	1.66
53	3	4		1648.2	1647.6	1652.6	0.677	0.64	1.10
	6	6		(1648.7)			0.075	0.07	0.08
54	0	2		1653.2	1652.6	1656.0	0.964	0.88	2.22
55			CI $g^3P–^3P_0$	1657.0	1656.6	1657.7			
56	4	5		1666.3	1665.8	1668.4	0.056	0.05	
57	1	3		1669.8	1669.2	1673.8	0.608	0.57	1.14
58	5	6		1685.1	1684.4	1686.5	0.038	0.04	
59	6	7		1704.5	1703.8	1709.9	0.098	0.09	0.13
	3	5		1705.4			0.406	0.38	0.69
60	0	3		1712.4	1710.9	1715.9	0.565	0.52	1.08
61	4	6		1724.1	1723.4	1728.4	0.376	0.36	
	7	8		1724.6			0.042		
62	1	4		1729.6	1728.4	1734.7	1.029	0.96	
63	5	7		1743.4	1742.8	1746.5	0.084	0.08	
64	2	5		1747.5	1746.8	1751.4	0.444	0.42	
65			CI $^1S–^1P^0$	1751.8	1750.9	1752.1			
66			CII $^2D–^2P^0$	1760.5	1760.0	1761.2			
67	0	4		1775.1	1774.5	1778.7	0.212	0.19	
68	4	7		1785.2	1784.6	1787.8	0.119	0.11	
69	1	5		1792.8	1792.1	1797.3	0.844	0.78	
70	5	8		1805.0	1804.4	1807.3	0.134	0.13	
	8	10		1805.6			0.014		
71	2	6		1811.4	1810.2	1815.0	0.827	0.78	
72	6	9		1825.6	1825.0	1825.9	0.051	0.05	
73	3	7		1830.2	1829.3	1829.9	0.279	0.26	
74	0	5		1841.7	1840.8	1843.8	0.048	0.04	
75	1	6		1859.9	1859.2	1863.9	0.326	0.30	
76	2	7		1878.7	1877.7	1883.4	0.519	0.49	
77	3	8		1898.3	1897.5	1902.5	0.383	0.36	
78	7	11		(1913.5)	1912.1	1914.6	0.024		
79	4	9		1918.5	1917.7	1922.6	0.147	0.14	
80			CI $^1D–^1P^0$	1930.9	1930.0	1935.1			
	1	7		1931.2			0.096	0.09	
81	5	10		1939.5	1938.9	1941.2	0.022	0.02	
82	2	8		1950.5	1949.6	1953.6	0.214	0.20	
83	3	9		1970.6	1969.7	1973.9	0.238	0.22	
84	4	10		1991.4	1990.6	1994.8	0.165	0.16	
85	1	8		(2007.2)	2006.3	2008.5	0.025	0.02	
86	5	11		2013.0	2012.1	2015.4	0.072	0.07	
87	2	9		2027.0	2026.2	2029.2	0.070	0.07	
88	6	12		(2035.4)	2034.8	2036.8	0.019	0.02	

4. The electronic transition moment of the CO A $^1\Pi$ - X$^1\Sigma$ band system

For diatomic molecules in an electronically excited state, the number of photons emitted per unit volume per second in a transition from the v' upper vibrational level to the v'' lower vibrational level (Shemansky et al. 1995) is

$$I_{v'v''} = n_{v'} A_{v'v''} \quad (2)$$

where n $_{v'}$ is the number density in level v' and

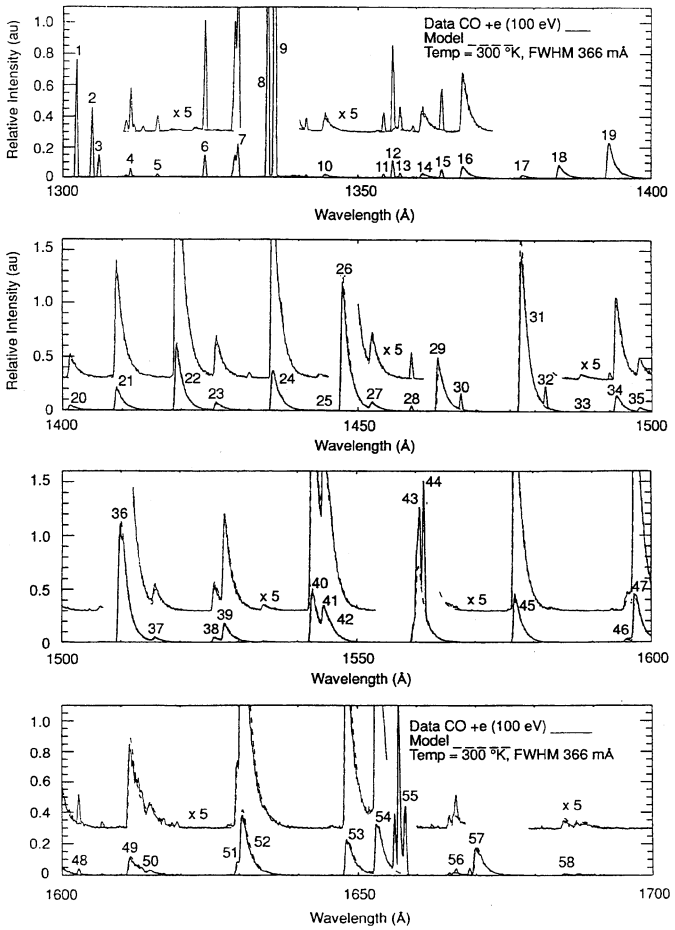

Fig. 2. Optically thin spectra of the CO (A-X) Fourth Positive band system between 1300 and 1700 Å (solid line) obtained with a cesium iodide coated channeltron detector at 100 eV electron impact energy and the corresponding model (dashed line).

$$A_{v'v''} = q_{v'v''}\nu^3_{v'v''}g[R^2_e(r_{v'v''})](2.03\times10^{-6}) \quad (3)$$

is the band transition probability. Here, $q_{v'v''}$ is the Franck-Condon factor, $\nu_{v'v''}$ is the transition energy in cm^{-1}, g is the statistical weight factor (2-$\delta_{0,\Lambda'+\Lambda''}/2 - \delta_{0,\Lambda''}$), R_e ($r_{v'v''}$) is the electronic transition moment function, and $r_{v'v''}$ is the r-centroid for the vibronic transition considered. The Franck-Condon factors for the CO A-X system are derived from semi-classical RKR potentials using a computer program supplied by Telle & Telle 1982. The construction of vibrational overlap integrals requires accurate spectroscopic parameters for the X and A states, including high order (to 8) for both rotational and vibrational distortion constants. Spectroscopic constants given by Tilford & Simmons 1972 are used in the calculation for the A state, and by Huber & Herzberg 1979 and LeFloch 1991 for the X state.

Eq. (2) can be written in the form

$$I_{v'v''} = p_{v'}A_{v'v''}/A_{v'} \quad (4)$$

where $p_{v'}$ is the volumetric excitation rate for the v' level, and $A_{v'}$ is the total transition probability for each v' level. The value $p_{v'}$ is defined by

$$p_{v'} = F_e(\sigma^{excitation}_{v'} + \sigma^{cascade}_{v'})N_0 \quad (5)$$

where F_e is the electron flux, $\sigma^{excitation}_{v'}$ is the excitation cross section (which is proportional to $q_{v'0}R^2_e$ ($r_{v'0}$),and N_0 is the gas density. $\sigma^{cascade}_{v'}$ is the total cascade cross section to level v' defined by a sum over all upper states, i, that are connected to the A state by known cascade vibrational transitions $v''' \rightarrow v'$ with the form

$$\sigma^{cascade}_{v'} = \Sigma\sigma^i_{v'''}A^i_{v'''v'}/A^i_{v'''} \quad (6)$$

For the A state the cascade transitions arise from the upper states B $^1\Sigma^+$ (v''' = 0) and C $^1\Sigma^+$ (v''' = 0) only.

We show in the next section that, to within 3%,

$$\sigma^{cascade}_{v'} \approx 0.06\sigma^{excitation}_{v'} \quad (7)$$

for all v' at 100 eV. At this energy we find that the array

$$\sigma^{cascade}_{v'}/\sigma^{excitation}_{v'} = [0.090, 0.077, 0.068, 0.060, 0.055, 0.049, 0.044]$$

for v' = 0 to 6, inclusive.

In order to obtain an absolute value for the transition moment we utilized the r-centroid approximation relation:

$$f_{v'v''} = 3.038\times10^{-6}q_{v'v''}g\nu_{v'v''}R^2_e(r_{v'v''}) \quad (8)$$

where $f_{v'v''}$ is the oscillator strength. Jolly et al. 1997 point out that this relationship is not valid for $v' > 12$ due to a breakdown of the r-centroid approximation for these high v'. Combining Eqs. (2) and (3) gives the relationship

$$R_e(r_{v'v''}) = [(constant/n_{v'}\nu^3_{v'v''}q_{v'v''})I_{v'v''}]^{1/2} \quad (9)$$

where the only unknown is $n_{v'}$. This requires another normalization procedure to obtain $R_e(r_{v',v''})$ in absolute units. The measured oscillator strengths published by Chan et al. 1993 (and recommended by Morton & Noreau 1994) for all transitions from $v' < 8$ to $v'' = 0$ were used to obtain an absolute $R_e(r_{v',v''})$ in Eq. (8) and compared with the measured intensities in Eq. (9) to generate the number density. Using this value of $n_{v'}$ we determined the values of $R_e(r_{v',v''})$ for $v'' \neq 0$ in units of Debye (1 a.u. $= ea_0 = 2.541\times10^{-18}$ esu = 2.541 D). The resulting values of R_e ($r_{v'v''}$) are plotted as a function of $r_{v'v''}$ in Fig. 3, together with previously reported experimental and theoretical data.

There is good agreement between the experimental data and the theoretical calculations of $R_e(r_{v'v''})$ shown in Fig. 3 in the region between 1.1 and 1.25 Å. In the r- centroid region $<$ 1.1 Å the values of De Leon 1989, Field et al. 1983 and Eidelsberg et al. 1992 are much higher than those of Chan et al. 1993, Spielfiedel et al. 1998, Kirby & Cooper 1989, Smith et al. 1994 and Jolly et al. 1997. The values calculated by Chantranupong et al. 1992 tend to fall in the middle of the two other groups. Our work tends

Table 2. Absolute transition probabilities of the A-X transition in units of 10^{+7} sec^{-1}. Values in parentheses were generated using the model. Values of (0.00) correspond to transition probabilities of less then 10^{+5} sec^{-1}

	v''= 0	1	2	3	4	5	6	7	8	9	10	11	Av'
v'=													
0	2.29	4.65	4.00	2.34	0.88	0.20	(0.04)	(0.01)	(0.00)	(0.00)	(0.00)	(0.00)	14.41
1	5.18	2.25	(0.03)	1.09	1.86	1.52	0.59	0.17	(0.05)	(0.10)	(0.02)	(0.00)	12.86
2	6.20	0.13	1.60	1.57	(0.04)	0.67	0.78	0.79	0.32	0.11	(0.19)	(0.00)	12.40
3	5.58	0.67	2.01	(0.00)	1.37	0.92	(0.00)	0.51	0.70	0.43	(0.50)	(0.05)	12.74
4	4.04	3.18	0.60	1.25	0.75	0.15	1.00	0.32	(0.04)	0.46	0.44	(0.28)	12.51
5	2.52	4.58	0.06	1.83	(0.01)	1.35	0.19	0.41	0.66	(0.07)	0.11	0.35	12.14
6	1.45	4.44	1.49	0.69	0.92	0.57	0.65	0.84	(0.00)	0.44	(0.31)	(0.00)	11.80
7	0.77	3.70	2.98	(0.00)	1.48	(0.04)	1.15	(0.00)	0.74	(0.21)	(0.11)	0.43	11.61

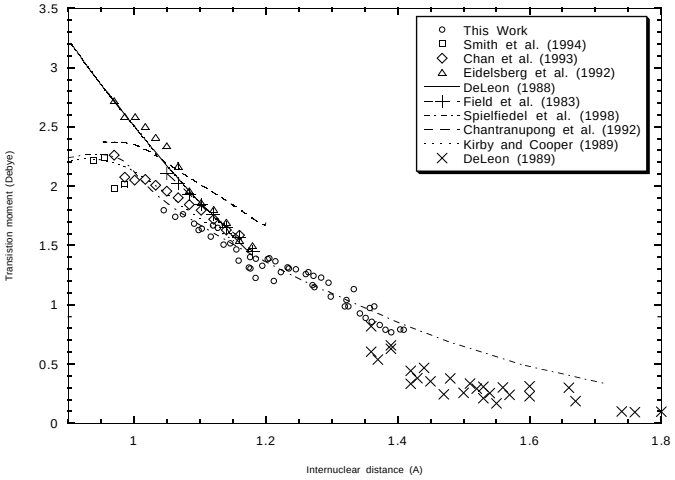

Fig. 3. Transition moment of the CO Fourth Positive band system. Included are values from this work (circles) and recently published fits (see text).

to be in excellent agreement with Spielfiedel et al. 1998, and within 5% of Chan et al. 1993, Smith et al. 1994, and Kirby & Cooper 1989.

The $R_e(r_{v'v''})$ values of De Leon 1989 are 23% less than our data in the r-centroid region between 1.3 and 1.4 Å. When we normalize the DeLeon(1989) data to ours in this region (by applying a scaling factor of 1.3) and generate a parabolic fit to the composite data set we obtain an electronic dipole moment function of the form:

$$R_e = 7.64(1 - 0.957 r_{v'v''} + 0.2247 r^2_{v'v''}) \quad (10)$$

Using the calculated $q_{v'v''}$ values and the experimental $R_e(r_{v'v''})$ values we have tabulated the band transition probabilities, $A_{v'v''}$ in Table 2 derived using Eq. 3. For $v' > 0$, the resulting $A_{v'v''}$ values tend to be $\sim$20% greater than those of Mumma et al. 1971. Within experimental error, this discrepancy can be explained by the low values for $A_{v'=2}$ (Hesser 1968; Wells & Isler 1970) which were used by Mumma et al. 1971 to normalize their data. However, our $A_{v'}$ value for the v' = 0 transitions is $\sim$35% higher than that of (Mumma et al. 1971). This is probably the result of some self absorption in our measured (0,0) resonance band that was used to obtain the absolute $R_e(r_{0,0})$ value to which our other $A_{0,v''}$ values were normalized. To verify this we calculated $A_{v'=0}$ using Eq. 3, the r-centroid values for v' to $v'' \neq 0$ transitions, and Eq. 10. The resulting value of $A_{v'=0}$ decreased from 14.41 ($10^{+7} sec^{-1}$) reported in Tables 2 to 13.2 ($10^{+7} sec^{-1}$).This represents a 24% increase, compared to the published value of Mumma et al. 1971, which is consistent with the differences between our values and those of Mumma et al. 1971 found for the other $A_{v'}$ values in Table 2

5. High resolution spectra of CO (A-X) (5,1) and (3,0) bands

In rotational fine structure we have shown (Ciocca et al. 1997a; Ajello et al. 1998) that

$$I_{v'v''J'J''} = p_{v'J'} A_{v'v''J'J''} / A_{v'} \quad (11)$$

where $I_{v'v''J'J''}$ is the rotational line intensity for the transition from the v', J' upper rovibronic level to the v'', J'' lower rovibronic level. The rotational-vibrational transition probability, $A_{v'v''J'J''}$, is separated into a product of a Hönl-London factor and a band transition probability (assuming negligible interaction between electronic and rotational motion). By means of this approximation Eq. 11 was used to generate the medium resolution model spectra in Figs. 1 and 2, including the measured value of R^2_e ($r_{v'v''}$) from this experiment.

The fit of the medium resolution spectra is excellent using Eq. 11 and the excitation rate derived from Eq. 5 and Eq. 7. The fact that cascade does not preferentially populate any particular v' to a significant degree makes the shape of the measured CO (A-X) spectra essentially the same as those from direct excitation without consideration of cascade. The rotational structure has a FWHM $\sim$2 Å at experimental temperatures and clearly needs to be modeled in order to match the laboratory spectra. The derived R^2_e ($r_{v'v''}$) from our experiment allows us to fit the laboratory spectra over the entire range from 1300–2050 Å.

In addition, we have obtained high resolution ($\sim$34 mÅ FWHM) second order spectra of the CO (A-X) (5,1) band at 1435 Å and the (3,0) band at 1447 Å, which are shown in Figs. 4a and 5a, respectively. The experimental conditions were selected to minimize self absorption in the (3,0) band by recording spectra at 4×10^{-5} torr, compared to 2×10^{-4} torr for the (5,1) band. The optical depth at 4×10^{-5} torr is less than 0.18 for

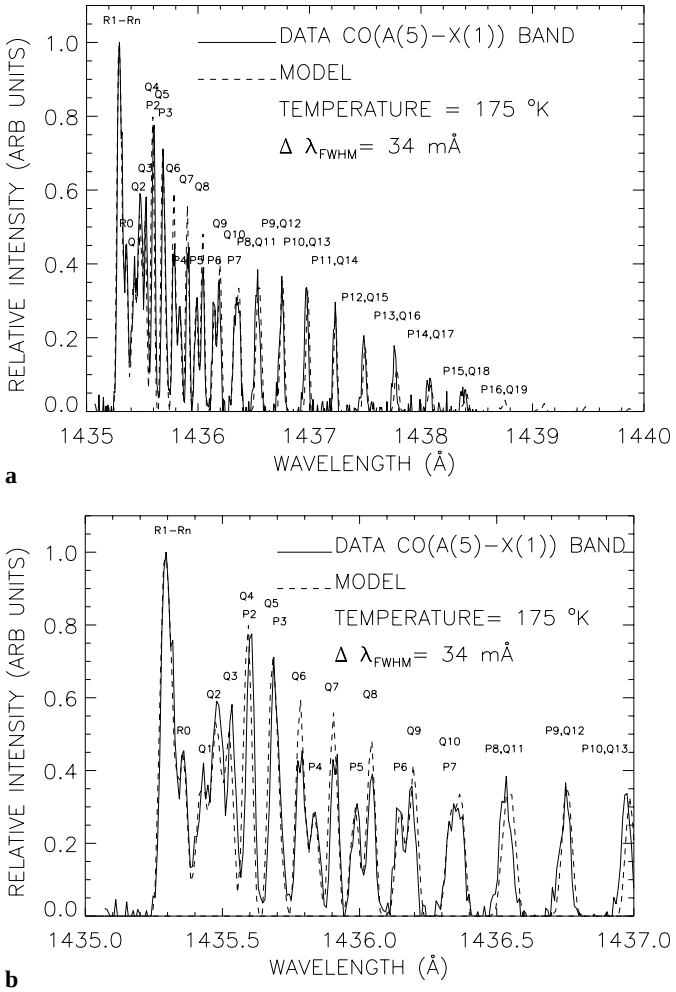

Fig. 4a and b. High resolution spectrum of CO (A-X) (5,1) band data (solid) and model (dash) normalized to unity at the R-branch head. **a** The wavelength range is 1435 to 1440 Å and **b** the wavelength range is 1435 to 1437 Å. The FWHM is 34 mÅ.

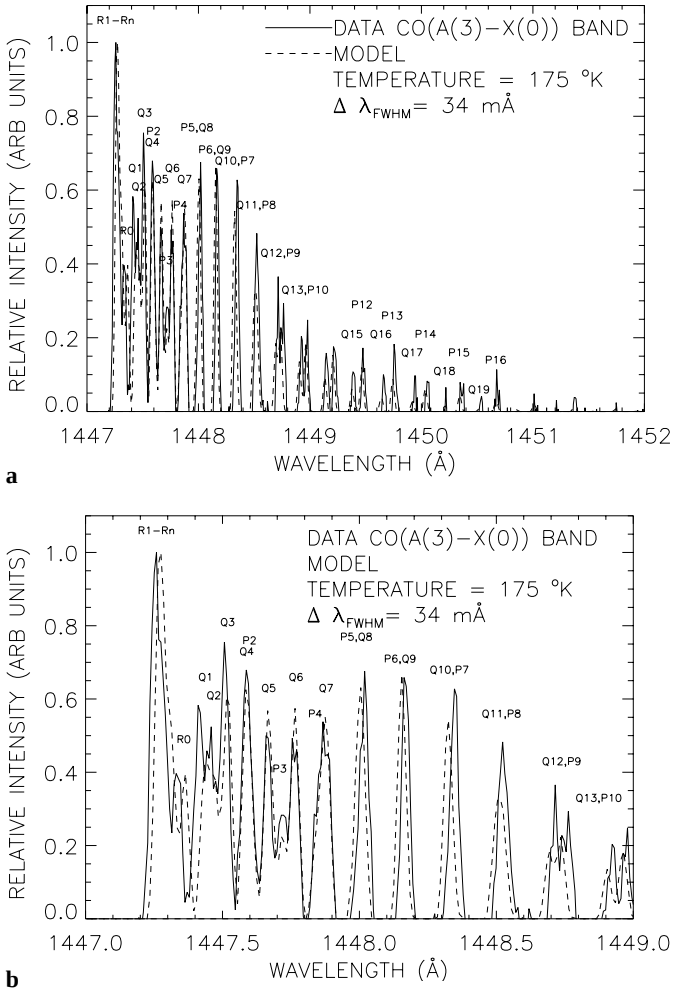

Fig. 5a and b. High resolution spectrum of CO (A-X) (3,0) band data (solid) and model (dash) normalized to unity at the R-branch head. **a** The wavelength range is 1447 to 1452 Å and **b** the wavelength range is 1447 to 1449 Å The FWHM is 34 mÅ.

the 5(3,0)Q rotational line at 175 K. The model from Eq. 11 accurately generates the rotational line structure consisting of P, Q and R-branches. The spectra are shown again in Figs. 4b and 5b with an expanded wavelength scale. The v' =3 and 5 levels are only very slightly perturbed (Field et al. 1983). The percentage character of perturbations based on singlet-triplet interaction is 0.3% from the d $^3\Delta$ state for v' =3, and 0.42% from the e $^3\Sigma^-$ state for v' =5. In each case the rotational constants form an R-branch head and allow a fit to the P and Q-branch data which are resolved. The details of the model for the (5,1) band lead to the determination of the rotational temperature of 175±25 K. The expanded model for the (3,0) band shows the effect of a small amount of self absorption for Q3-Q7. The (5,1) model fits the data to better than 10% except for the Q6 and Q7 features where a 20% discrepancy is found. Small shifts in wavelength of $\sim$10 mÅ occur because of temporal temperature variations of the spectrometer of $\sim$0.1 K over the 3 days of spectral data acquisition.

6. Excitation function of the A $^1\Pi$ - X $^1\Sigma$ (0,1) band

The energy dependence of the CO A $^1\Pi$ cross section was studied by measuring the excitation function of the strong A $^1\Pi$ (v' =0) - X $^1\Sigma^+$ (v''=1) band at 1597 Å in the electron impact energy range from threshold to 750 eV. Measurements were performed at a spectral resolution of 2.9 Å (FWHM) and at a gas pressure of 1×10^{-4} torr. Relative excitation function data were put on an absolute scale by normalizing the intensity at 100 eV to an emission cross section value of 1.12×10^{-18} cm^2, measured using the relative flow technique (described in Sect. 2). The excitation function data are plotted in Fig. 6, together with renormalized measurements of Aarts & de Heer 1970, Mumma et al. 1971 and Ajello 1971a, as described later.

The relationship between the measured emission cross section for the CO (A-X) (0,1) band ($\sigma_{0,1}^{emission}$) and the cross section for direct excitation of the A $^1\Pi$ v'=0 level ($\sigma_0^{excitation}$) is given by:

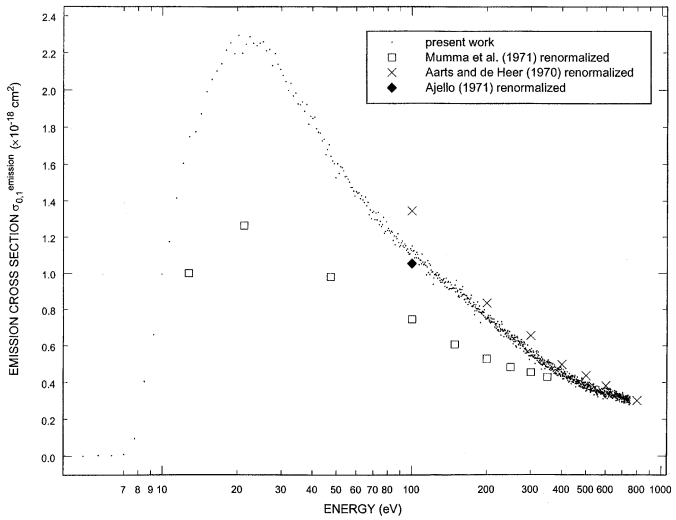

Fig. 6. Emission cross section of the CO (A-X) (0,1) transition at 1597 Å (dots). The previous measurements of Aarts & de Heer 1970 (crosses), Mumma et al. 1971 (Squares) and Ajello 1971a (Diamond) have been renormalized, as described in the text.

$$\sigma_{0,1}^{emission} = (A_{0,1}/A_0)[\sigma_0^{excitation} + \sigma_0^{cascade}] \qquad (12)$$

where ($A_{0,1}$ / A_0) is the emission branching ratio calculated from the ratio of transition probabilities $A_{v'v''}$ given in Table 2 and has a value of 0.3237, $A_0 = \Sigma_{v''}(A_{0,v''})$ and $\sigma_0^{cascade}$ is the total cascade cross section for decay from higher-lying B $^1\Sigma^+$ and C $^1\Sigma^+$ states to the v' = 0 level of A $^1\Pi$ state.

Excitation of the B $^1\Sigma^+$ and C $^1\Sigma^+$ states was studied in our earlier publications (James et al. 1992, Kanik et al. 1995). Unlike the A $^1\Pi$ state, the B and C states have approximately the same equilibrium internuclear distances as the X $^1\Sigma^+$ ground state and hence only their v' = 0 vibrational levels are populated to any significant degree in the excitation process. Decay from the B $^1\Sigma^+$ state to the A $^1\Pi$ state via the (B-A) Angstrom band system in the visible spectral region represents 40% of the total emission from the B state. Similarly, decay from the C $^1\Sigma^+$ state to the A $^1\Pi$ state via the (C-A) Herzberg band system represents 7% of the total emission from the C state (Letzelter et al. 1987). The only other radiative decay channels available to the B or C states are direct EUV transitions to the X $^1\Sigma^+$ ground state. Non-radiative process (dissociation, photodissociation) are found to be 0% for the B(0) level and <10% for the C(0) level (Letzelter et al. 1987). It should be noted that the shape of the B-X (0,0) excitation function exhibits an anomalously sharp peak at low energy not typically characteristic of such a dipole-allowed transition. This may be caused by spin exchange from a significant triplet admixture. The unusually large branching ratio for the visible Ångstrom bands (B-A) arises from the large dipole moment between the B and A states (Kirby and Cooper, 1989).

In order to calculate the cascade cross section in Eq. 12 for v' = 0, our previous measurements of the excitation functions of the (B-X) (0,0) and (C-X) (0,0) bands (Kanik et al. 1995) were firstly scaled by factors of 0.4 and 0.07, respectively, to yield the total (B-A) and (C-A) cascade cross sections, as shown in Fig. 7.

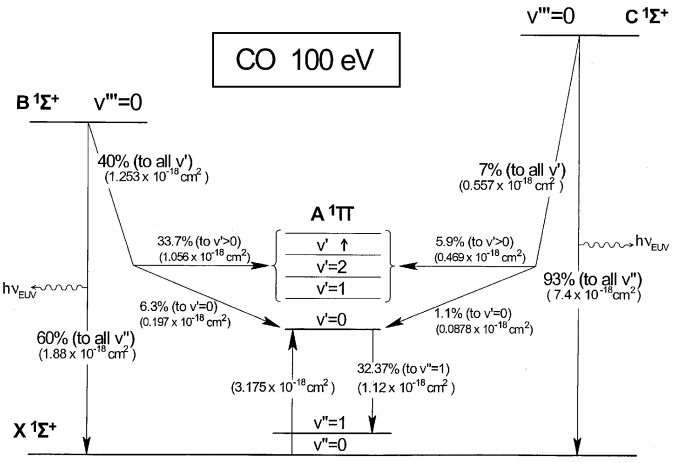

Fig. 7. Diagram of the direct, cascade and emission processes and associated branching ratios used to derive cross sections of the A(0) state. Branching ratios are indicated as a percentage, and associated cross sections at 100 eV are given in parentheses.

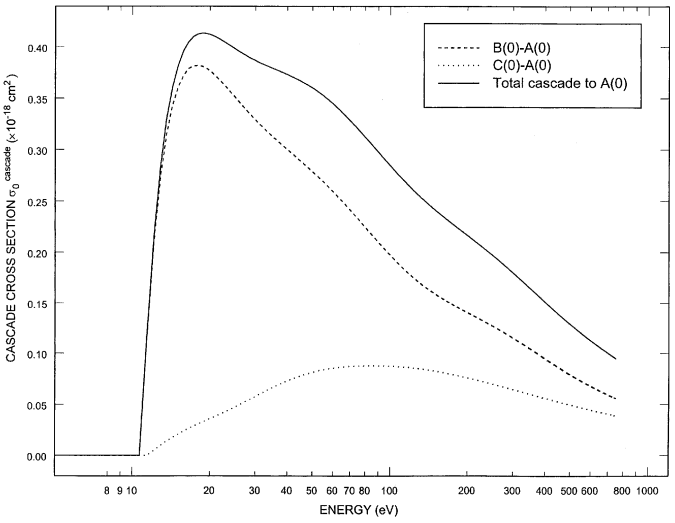

Fig. 8. Cross sections for cascade from higher-lying B and C states to the A (v' = 0) level, calculated as described in the text. The total cascade is the sum of contributions from B(0) and C(0) to A(0).

Partitioning these scaled excitation functions by the additional branching ratio $(q_{0,0}/\lambda_{0,0}^3)/(\Sigma_{v''}[q_{0,v''}/\lambda_{0,v''}^3])$ generates the total cascade contributions to the v' = 0 level of the A $^1\Pi$ state ($\sigma_0^{cascade}$) shown in Fig. 8. The Franck-Condon factors ($q_{0,v''}$) and corresponding transition wavelengths ($\lambda_{0,v''}$) are listed by Krupenie 1966 for the (B-A) (0,v'') and (C-A) (0,v'') systems, and a constant electronic transition moment was assumed. Note that the net cascade contribution to the measured (A-X) (0,1) excitation function can be obtained by further partitioning this value by our measured (0,1) emission branching ratio ($A_{0,1}$ / A_0) of 0.3237. The direct, cascade and emission processes and associated branching ratios used to derive cross sections for the A(0) state are summarized in Fig. 7. The two sets of branching ratios used to calculate the cascade cross section are indicated, together with the emission branching ratio ($A_{0,1}$ / A_0) of 0.3237.

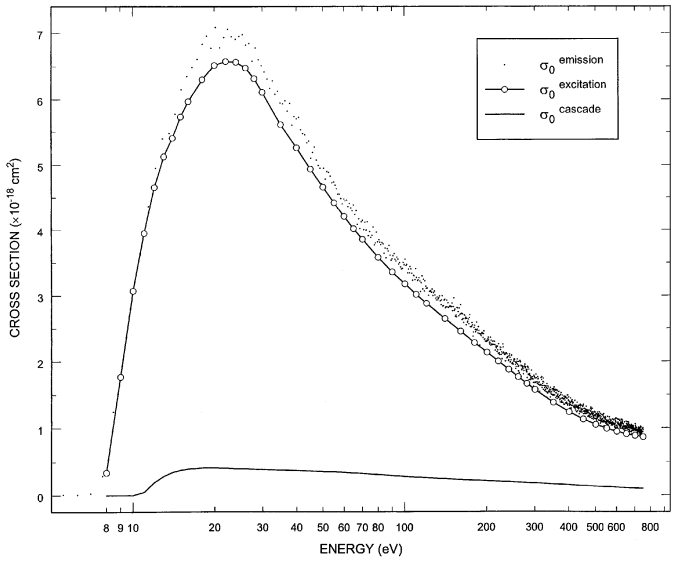

Fig. 9. Measured experimental emission (dots) and calculated excitation (line-cicrle) cross sections of the A ($v' = 0$) level in the energy range from threshold to 750 eV showing the calculated cascade contribution (line) from higher-lying B and C states.

Fig. 9 shows $\sigma_0^{excitation}$, $\sigma_0^{cascade}$, and $\sigma_0^{emission}$ for the A $^1\Pi$ v' =0 level calculated using Eq. 12. Representative values of these cross sections are listed in Table 3 as a function of electron impact energy. At 100 eV, for example, $\sigma_0^{excitation}$, $\sigma_0^{cascade}$, and $\sigma_0^{emission}$ are 3.175, 0.285, and 3.46×10^{-18} cm^2, respectively. The ratio of the cascade to direct excitation cross sections for the A $^1\Pi$ v' = 0 level ($\sigma_0^{cascade}$ /$\sigma_0^{excitation}$) ranges from ∼5% at ∼30 eV to a maximum of ∼11% at ∼500 eV.

The cross section for direct excitation of the v' level of a state from the v' =0 ground state ($\sigma_{v'}^{excitation}$) is related to the Franck-Condon factor ($q_{v'0}$) and electronic transition moment ($R_e(r_{v'0})$) via:

$$\sigma_{v'}^{excitation} \propto q_{v'0} R_e^2(r_{v'0}) \quad (13)$$

Based on the (A-X) Franck-Condon factors (calculated from an RKR potential using the programs developed by Telle & Telle 1982) and the present measurements of electronic transition moments, Eq. 13 indicates that $\sigma_{0,1}^{excitation}$ represents 11.53% of the total A $^1\Pi$ excitation cross section ($\sigma_{total}^{excitation}$). Thus $\sigma_{total}^{excitation}$ = $\sigma_{0,1}^{excitation}$ / 0.1153. The total cascade contribution summed over all v' levels of the A $^1\Pi$ state ($\sigma_{total}^{cascade}$) can be obtained by dividing $\sigma_0^{cascade}$ by the branching ratio ($q_{0,0}$ / $\lambda_{0,0}^3$) / ($\Sigma_{v''}$ [$q_{0,v''}$ / $\lambda_{0,v''}^3$]) initially used to partition it, as described above. Finally, the total emission cross section from all v' levels of the A $^1\Pi$ state ($\sigma_{total}^{emission}$) is given by the sum of $\sigma_{total}^{excitation}$ and $\sigma_{total}^{cascade}$. Fig. 10 shows $\sigma_{total}^{excitation}$, $\sigma_{total}^{cascade}$, and $\sigma_{total}^{emission}$ for the A $^1\Pi$ state (summed over v'). Representative values of these cross sections are listed in Table 4 as a function of electron impact energy. At 100 eV, for example, $\sigma_{total}^{excitation}$, $\sigma_{total}^{cascade}$, and $\sigma_{total}^{emission}$ for the A$^1\Pi$ state are 27.55, 1.81, and 29.36×10^{-18} cm^2, respectively. The latter value is in experimental agreement with a corrected value (described below) for $\sigma_{total}^{emission}$ at 100 eV of 28×10^{-18} cm^2 measured in the earlier low resolution experiment of Ajello 1971a. Our value for $\sigma_{total}^{emission}$ at 100 eV obtained from the analysis of the (0,1) excitation function (29.36×10^{-18} cm^2) is ∼16% lower than the value of 35.1×10^{-18} cm^2 derived by summing the intensities of all bands observed in our 100 eV spectra (as described in Sect. 3). This discrepancy can be explained by errors in the

Table 3. Cross sections for the A $^1\Pi(v' = 0)$ level.

Energy (eV)	$\sigma_0^{excitation}$ (x10^{-18} cm^2)	$\sigma_0^{cascade}$ (10^{-18} cm^2)	$\sigma_0^{emission}$ (x10^{-18} cm^2)
8	0.341	0.000	0.341
9	1.770	0.000	1.770
10	3.073	0.000	3.073
11	3.953	0.046	4.000
12	4.662	0.200	4.862
13	5.129	0.293	5.422
14	5.407	0.348	5.755
15	5.738	0.381	6.119
16	5.969	0.399	6.368
18	6.300	0.413	6.713
20	6.518	0.412	6.930
22	6.578	0.407	6.985
24	6.566	0.401	6.967
26	6.477	0.396	6.873
28	6.312	0.391	6.703
30	6.109	0.387	6.496
35	5.615	0.379	5.995
40	5.259	0.373	5.632
45	4.941	0.367	5.308
50	4.663	0.360	5.023
55	4.420	0.353	4.773
60	4.208	0.345	4.553
65	4.022	0.337	4.359
70	3.858	0.329	4.187
80	3.582	0.313	3.895
90	3.360	0.298	3.658
100	3.175	0.285	3.460
110	3.018	0.273	3.291
120	2.881	0.264	3.145
140	2.650	0.248	2.898
160	2.456	0.236	2.692
180	2.287	0.226	2.513
200	2.137	0.217	2.354
220	2.001	0.209	2.210
240	1.878	0.201	2.080
260	1.767	0.194	1.961
280	1.666	0.187	1.852
300	1.574	0.180	1.754
350	1.383	0.165	1.548
400	1.238	0.151	1.389
450	1.130	0.139	1.269
500	1.049	0.129	1.178
550	0.990	0.120	1.110
600	0.945	0.113	1.058
650	0.911	0.106	1.017
700	0.884	0.100	0.985
750	0.863	0.095	0.958

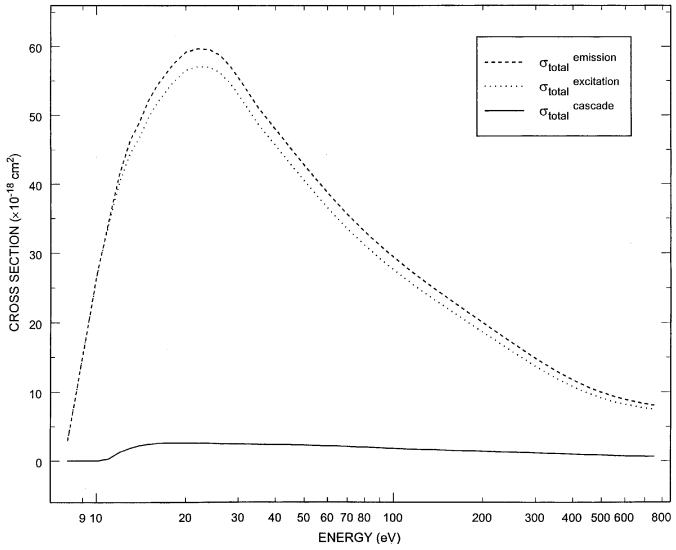

Fig. 10. Total calculated emission (dash) and excitation (dots) cross sections of the Fourth Positive band system in the energy range from threshold to 750 eV, including the total cascade cross section (line) from higher-lying B and C states.

relative spectral sensitivity calibration, branching ratios, signal statistics etc. and is within our stated error bar of 25%.

Measurements of the excitation function of the (A-X) (0,1) band in the energy range from 100 to 5000 eV were carried out by Aarts & de Heer 1970. They used the (A-X) $f_{0,0}$ oscillator strength measured by Lassettre & Skerbele 1971 to calculate $\sigma_0^{excitation}$ and then obtained $\sigma_{0,1}^{emission}$ using an emission branching ratio of 0.289 determined assuming a constant electronic transition moment. The oscillator strength of Lassettre & Skerbele 1971 used by Aarts & de Heer 1970 to normalize their data is $\sim$12% higher than the recommended value given by Morton & Noreau 1994. However, the emission branching ratio assumed by Aarts & de Heer 1970 was $\sim$11% lower than that measured in the present work. Fortuitously, rescaling the original Aarts & de Heer 1970 data to reflect these two changes leaves their original values essentially unchanged (and $\sim$21% higher than the present value at 100 eV). A correction to reflect the decrease in the adopted oscillator strength was also applied to the $\sigma_{total}^{emission}$ data of Ajello 1971a, who normalized his result to Aarts & de Heer 1970. The latter authors estimated $\sigma_0^{cascade}$ to be only 1.5% of $\sigma_0^{emission}$. The emission branching ratio of 0.14 assumed by Aarts and de Heer (1970) for the (B-A) channel lowers their estimated cascade contribution from the (B-A) bands by nearly a factor of 3 over the present calculations.

Mumma et al. 1971 measured the (A-X) (0,1) excitation function in the energy range from near-threshold to 350 eV and rescaled the cross section values of Aarts & de Heer 1970 higher by a factor of 1.115 in order to correct for the non-constant electronic transition moment (see Sect. 3). Mumma et al. 1971 also concluded that cascade effects are unimportant for the calculation of relative (A-X) band intensities. The benchmark cross section for dissociative excitation of H_2 Lyman-α used by Mumma et al. 1971 to calibrate their relative spectral data has subsequently been revised lower by a factor of 0.61 (Ajello et al. 1988). This indicates that the original data of Mumma et al. 1971 overestimated the cross section by $\sim$64%. The Mumma et al. 1971 data were rescaled to reflect this decrease in the H_2 Lyman-α cross section. The renormalized Aarts & de Heer 1970, Mumma et al. 1971 and

Table 4. Total cross sections for the CO Fourth Positive (A-X) system.

Energy (eV)	$\sigma_{total}^{excitation}$ (x10^{-18} cm^2)	$\sigma_{total}^{cascade}$ (10^{-18} cm^2)	$\sigma_{total}^{emission}$ (x10^{-18} cm^2)
8	2.96	0.00	2.96
9	15.35	0.00	15.35
10	26.66	0.00	26.66
11	34.30	0.29	34.59
12	40.44	1.27	41.71
13	44.50	1.86	46.36
14	46.91	2.21	49.12
15	49.78	2.42	52.20
16	51.79	2.53	54.32
18	54.66	2.62	57.28
20	56.55	2.62	59.17
22	57.07	2.59	59.66
24	56.97	2.55	59.52
26	56.20	2.51	58.71
28	54.77	2.48	57.25
30	53.01	2.46	55.46
35	48.72	2.41	51.13
40	45.63	2.37	48.00
45	42.87	2.33	45.20
50	40.46	2.29	42.75
55	38.35	2.24	40.59
60	36.51	2.19	38.70
65	34.90	2.14	37.04
70	33.47	2.09	35.56
80	31.08	1.98	33.07
90	29.15	1.89	31.04
100	27.55	1.81	29.36
110	26.18	1.74	27.92
120	25.00	1.67	26.67
140	22.99	1.57	24.56
160	21.31	1.50	22.81
180	19.85	1.43	21.28
200	18.54	1.38	19.92
220	17.36	1.33	18.69
240	16.30	1.28	17.57
260	15.33	1.23	16.56
280	14.45	1.19	15.64
300	13.66	1.14	14.80
350	12.00	1.04	13.04
400	10.74	0.96	11.70
450	9.80	0.88	10.69
500	9.10	0.82	9.92
550	8.59	0.76	9.35
600	8.20	0.72	8.91
650	7.90	0.67	8.58
700	7.67	0.64	8.31

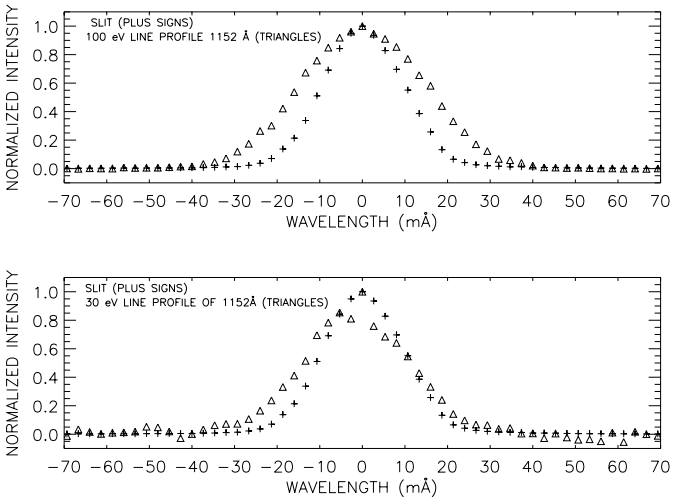

Fig. 11a and b. High resolution experimental line profile spectrum of OI ($^1D \leftarrow^1 D^o$) at 1152.16 Å (triangles) and the instrumental slit function(plus signs) at 22 mÅ FWHM in third order at **a** 100 eV and **b** 30 eV. The step size was 2.667 mÅ/channel. The background pressure was 1×10^{-4} Torr with an electron beam current of 200 μA.

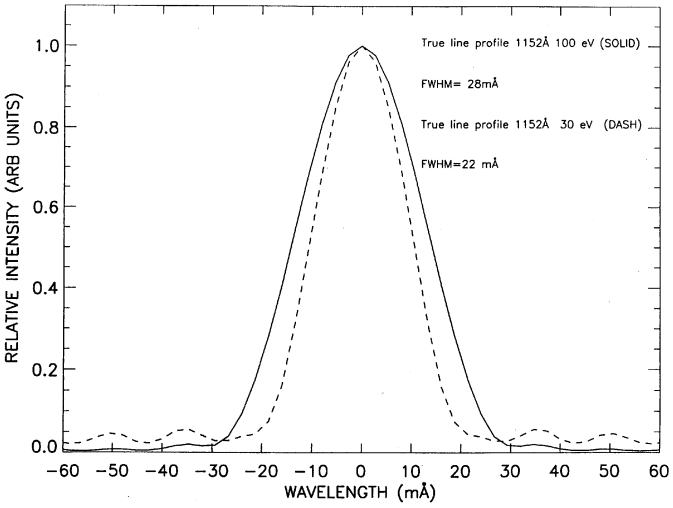

Fig. 12. Deconvolution of the 30 eV (dash) and 100eV (solid) line profiles from the measured profiles of Fig. 11 using a FFT technique.

Ajello 1971a $\sigma_{0,1}^{emission}$ data are plotted in Fig. 6, and show significant differences in the shape functions for these data sets.

Recent measurements of Zetner et al. 1998 using the electron energy loss technique at 3 energies (10, 12.5 and 15 eV) fall well within the error bars of our total cross section determination of the CO Fourth Positive band system.

Finally, the oscillator strength ($f_{0,0}$) for excitation of the v' =0 level of the A $^1\Pi$ state was derived from the gradient of the high energy asymptotic slope of a 'Bethe-Fano' plot of the collision strength ($\sigma_0^{excitation}$ * Energy) vs. log (Energy). A value of 0.0155±0.001 was obtained, in experimental agreement with the Chan et al. 1993 and Zhong et al. 1997 values of 0.0162 and 0.0166, respectively, derived from electron energy loss measurements.

7. Line profile study of OI(1152.16 Å) from dissociative excitation of CO

Measurements of Doppler emission line profiles at high optical resolution can provide information on the kinetic energy distributions of atoms from dissociative excitation of a molecule. The electron-impact-induced fluorescence line profiles of OI ($^1D \leftarrow^1 D^o$) at 1152.16 Å produced by dissociative excitation of CO at 100 eV and 30 eV are shown in the high resolution spectra in Fig. 11a and b, respectively, together with the instrumental slit function of the spectrometer. The measured line profiles are different at the two impact energies, with an indicated FWHM of 26 mÅ at 30 eV, broadening to 35 mÅ at 100 eV. This compares to the measured slit function with a FWHM of 22 mÅ. Data points are obtained every 2.6667 mÅ in single scans. Both the 30 eV and 100 eV profiles are symmetric. The line profiles were measured at an angle of 90° to both the electron and molecular beam axes.

Fast Fourier Transform (FFT) techniques were used to recover the actual line profile (Ajello & Ciocca 1996; Ciocca et al. 1997b). We selected a step filter to remove high frequency noise from the FFT of both the measured line profile and the slit function. The measured line profile is the convolution of the true line profile and the instrumental slit function. We show in Fig. 12 the two deconvolved true line profiles with a FWHM of 22±6 mÅ and 28±4 mÅ for the 30 eV and 100 eV OI (1152 Å) line profiles, respectively. The true line profiles, the measured line profiles and the slit function are all approximately Gaussian. The root-sum-square of the FWHM of the true line shape and the slit function should approximately equal the FWHM of the measured profile. This is found to be the case to within 1 mÅ for the 100 eV line profile and to within 4 mÅ for the 30 eV line profile. The uncertainties in the true line profiles are about 25% at 30 eV and about 12% at 100 eV.

For each of the line profiles in Fig. 12, the corresponding kinetic energy distribution of the fragments, P(E), is given by

$$P(E) = k(dT/d\lambda) \tag{14}$$

where k is a constant and T is the true line profile. The expression is exact if the distribution function is isotropic. The kinetic energy distributions of the OI(^{1}D) fragments at 30 eV and 100 eV are shown in Fig. 13. The fragment distribution of OI(^{1}D) atoms has a FWHM of 5±1 eV with a peak energy at 1.5±0.5 eV for 100 eV electron impact energy. The fragment distribution of OI(^{1}D) atoms has a FWHM of 3.0±0.5 eV with a peak value at 1.0±0.3 eV for 30 eV electron impact energy. The fragment population measured here extends to energies of 9 eV and 5 eV for 100 eV and 30 eV impact energies, respectively.

The calculated threshold in this experiment for the companion fragment atom (ion) to a OI(^{1} D) excited atom are: 1) 21.9 eV for a C(^{3} P) ground state atom and 2) 33.1 eV for a C^+ ($^2P^0$) ion. Thus the line profile at 30 eV arises exclusively from dissociative excitation, while the line profile at 100 eV consists of contributions from both dissociative excitation and

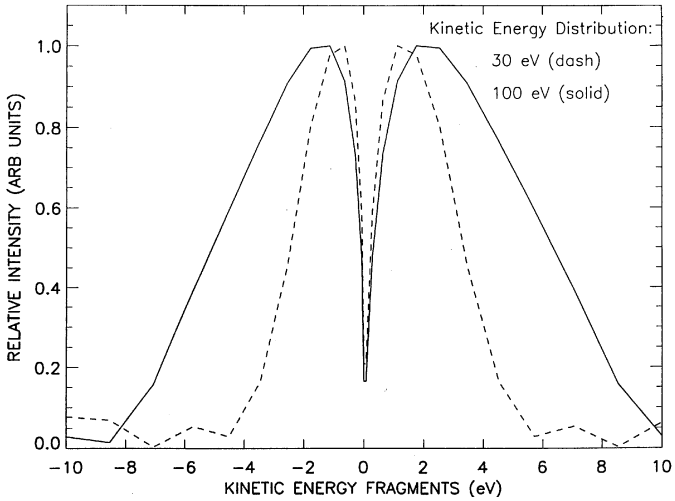

Fig. 13. Kinetic Energy distribution of OI(^{1} D) atoms at 30 eV (dash) and 100 eV(100 eV) from dissociative excitation of CO.

dissociative ionization excitation. The kinetic energy distributions of fragments in dissociation of CO from repulsive states is far from thermal. Dissociative ionization excitation produces faster OI(^{1}D) excited atoms, as was the case in our previous study of N_2 (Ajello & Ciocca 1996).

8. Discussion

The CO Fourth Positive band system plays a major role in the UV luminosity that originates in the atmospheric dayglow emissions on Mars and Venus. The atmospheres of both of these planets are dominated by CO_2. On Mars the number density ratio of CO_2/CO is of the order of 100 throughout the thermosphere. On Venus the CO_2 number density dominates over the CO number density in the lower atmosphere up to approximately 150 km at night, and 170 km in the day. At higher altitudes atomic O eventually becomes the major constituent in the upper atmospheres of both planets. This is a direct result of photodissociation and diffusive separation which allows CO and O to become more abundant at higher altitude.

The five sources of the CO Fourth Positive band spectrum include:

1. electron impact excitation of CO:

$$CO(X) + e \rightarrow CO(A) + e \quad (15)$$

2. fluorescent scattering by CO:

$$CO(X; v_1) + h\nu \rightarrow CO(A; v_2) \rightarrow CO(X; v_3) + h\nu' \quad (16)$$

3. electron impact dissociative excitation (or ionization excitation) of CO_2:

$$CO_2 + e \rightarrow CO(A) + O + e \quad (17)$$

4. photodissociative excitation (or photoionization excitation) of CO_2:

$$CO_2 + h\nu \rightarrow CO(A) + O \quad (18)$$

and 5) dissociative recombination of CO_2^+

$$CO_2^+ + e \rightarrow CO(A) + O \quad (19)$$

(Gutcheck & Zipf 1973 and Fox 1992)

A review of the creation mechanisms for the CO Fourth Positive band system, as well as other features observed in the atmospheres of Mars and Venus, can be found in Fox 1992 and references therein. Fox & Dalgarno 1979a found that the major sources of the CO (A-X) system on Mars were photodissociation or photoionization of CO_2 by solar radiation less than 1082 Å, and dissociative recombination of CO_2^+. On Venus the major source of the CO Fourth Positive band system was found to be fluorescent scattering (Fox & Dalgarno 1979b) which is 1.5 orders of magnitude stronger than electron impact excitation of CO, the next most important source.

Unlike in the solar system, emission from extra-solar system objects in the ISM has not been detected for CO. However, collisional excitation has been observed for the first time from H_2 in a Herbig-Haro object (Raymond et al. 1997).

The remeasurement of the electron impact cross sections performed in this work has improved the accuracy of the cross sections of most of the CO Fourth Positive bands when compared to the previous works of Aarts & de Heer 1970, Mumma et al. 1971 and Ajello 1971a and has thereby enabled more accurate calculations and modeling of aeronomical excitation values (process 1). Ajello 1971b states that the cross section of the A state of CO from dissociative excitation of CO_2 (process 3) is about a factor of 32 lower than the corresponding direct excitation cross section of the A state of CO. Since the calibration standards have been revised substantially lower since the measurements of Ajello 1971b and Mumma et al. 1975 on CO_2, it would be useful to go back and re-measure these CO_2 cross sections, especially considering their importance in planetary atmospheric modeling. However, at the present time, the results of this paper indicate that for Mars electron impact of CO and CO_2 produces similar signal levels since the cross sections are inverse to the number density ratios in the thermosphere.

The present determination of the electronic transition moment (R_e) as a function of internuclear distance ($r_{v'v''}$) is in particularly good agreement with the recent work of Spielfiedel et al. 1998, as well as being in agreement with Federman et al. 1997, Smith et al. 1994, Chan et al. 1993, and Kirby & Cooper 1989. The calculated absolute electronic transition moment leads to a direct calculation of the transition probability ($A_{v'v''}$) for the Fourth Positive band system from Eq. 3. For $v' > 0$, our $A_{v'v''}$ values are $\sim$20% greater than those of Mumma et al. 1971 due to the low value for $A_{v'=2}$ used by Mumma et al. 1971 to normalize their data. However, our $A_{v'}$ value for the v' = 0 transition is $\sim$35% higher than Mumma et al. 1971, probably due to some self absorption of the (0,0) resonance band in our spectra (which all other $A_{0v''}$ values are normalized to).

We constructed a model that explains the high resolution rotational fine structure of the CO (A-X) (3,0) and (5,1) bands. The spectra in Figs. 4 and 5 show this model in comparison with

the experimental spectra. There is evidence of some self absorption in the (3,0) bands for $J' \sim 7$. This slight self absorption can be modeled with an absorption term in Eq. 11. However, the simple model (involving the separation of rotational and electronic dipole moments into a product) allows accurate modeling of high resolution spectra of CO. The most highly perturbed vibrational level is expected to be v'' = 0 or 1 and extra rotational values are found.

Our remeasurement of the excitation function of the CO (A-X) (0,1) transition at 1597 Å undermines the nominally close agreement with the present data attained 30 years ago for the uncorrected cross sections from the three different experiments of Aarts & de Heer 1970, Mumma et al. 1971 and Ajello 1971a. The previous work has been renormalized (where appropriate) to reflect the decrease in both the benchmark UV emission cross sections and oscillator strengths used by these authors to normalize their data, and corrected for changes in the emission branching ratio. At 100 eV, for example, the (0,1) emission cross section measured here is $\sim$ 17% lower than the corrected data of Aarts & de Heer 1970, $\sim$ 50% higher than the corrected value of Mumma et al. 1971, and $\sim$ 10% higher than the corrected value of Ajello 1971a. The corrected value of Mumma et al. 1971 now lies outside our experimental error bar.

Finally, cascade from the higher lying B and C states to the A state was found to be a significant percentage of the total excitation cross section, varying from 9% for the v' = 0 level to 4% for v' = 6 at 100 eV. Fortunately, even though this is a significant fraction of the excitation, the cascade contributions remain relatively constant for all v' such that relative spectral intensities developed in the model were not significantly affected.

Acknowledgements. The research described in this paper was carried out at the Jet Propulsion Laboratory, California Institute of technology, and was sponsored by the NASA UV, Visible and Gravitational Astrophysics Program Office and Planetary Atmospheres Program Office, the U.S. Air Force Office of Scientific Research (AFOSR) and the Aeronomy Program of the National Science foundation (ATM-9320589). Three of us (L.W.B., M.A. and D.D.) are supported by the National Research Council through a Resident Research Associateship at the Jet Propulsion Laboratory, California Institute of Technology. The authors wish to acknowledge G. Stark, F. Launay and F. Rostas for their helpful comments and a critical reading of the manuscript. Finally, we thank the anonymous referee for critically reading the paper and for the thorough review.

References

Aarts J.F.M., de Heer F.J., 1970, J. Chem. Phys. 52, 3554
Ajello J.M., 1971a, J. Chem. Phys. 55, 3158
Ajello J.M., 1971b, J. Chem. Phys. 55, 3169
Ajello J.M., Ahmed S.M., Liu X., 1996, Phys. Rev. A 53, 2303
Ajello J.M., Ciocca M., 1996, J. Geo. Res. 101, 18953
Ajello J.M., James G.K., Franklin B.O., Shemansky D.E., 1989, Phys. Rev. A 40, 3524
Ajello J.M.,, Shemansky D.E., 1985, J. Geophys. Res. 90, 9845
Ajello J.M., Shemansky D.E., Franklin B., et al., 1988, Applied Optics 27, 890
Ajello J.M., James G., Ciocca M., 1998, J. Phys. B: At Mol Opt Phy 31, 1
Barth C.A., Stewart A.I.F., Brougher S.W., et al., 1992, In: Mars. University of Arizona Press, 1054
Bartoe J.D.F., Brueckner G.E., Sandlin G.D., VanHoosier M.E., Jordan C., 1978, ApJ 223, L51
Chan F., Cooper G., Brion C.E., 1993, Chem. Phys. 170, 123
Chantranupong L., Bhanuprakash K., Honigmann M., Hirsch G., Buenker R.J., 1992, Chem. Phys. 161, 351
Ciocca M., Kanik I., Ajello J.M., 1997a, Phys. Rev. A 55, 3547
Ciocca M., Ajello J.M., Liu X., 1997b, Phys. Rev. A 56, 1929
De Leon R.L., 1988, J. Chem. Phys. 89, 70
De Leon R.L., 1989, J. Chem. Phys. 91, 5859
van Dishoeck E.F., Black J.H., 1988, ApJ 334, 771
Eidelsberg M., Jolly A., Lemaire J.L., et al., 1998, A&A (in press)
Eidelsberg M., Rostas F., Breton J., Thieblemont B., 1992, J. Chem. Phys. 96, 5585
Federman S.R., Menningen K.L., Lee W., Stoll J.B., 1997, ApJ 477, L61
Field R.W., Benoist d'Azy O., Lavollée M., Lopez-Delgado R., Tramer A., 1983, J. Chem. Phys. 78, 2838
Fox J.L., 1992, In: Venus and Mars: Atmosphers, Ionospheres, and Solar Wind Interactions. American Geophysical Union 191
Fox J.L., Dalgarno A., 1979a, J. Geophys. Res. 84, 7315
Fox J.L., Dalgarno A., 1979b, J. Geophys. Res. 86, 629
Gutcheck R.A., Zipf E.C., 1973, J. Geophys. Res. 78, 5429
Hesser J.E., 1968, J. Chem. Phys. 48, 2518
Huber K.P., Herzberg G., 1979, Molecular Spectra and Molecular Structure: IV. Constants of Diatomic Molecules. Van Nostrand, New York
James G.K., Ajello J.M., Franklin B.O., Shemansky D.E., 1990, J. Phys. B 23, 2055
James G.K., Ajello J.M., Kanik I., Franklin B.O., Shemansky D.E., 1992, J. Phys. B 25, 1481
Jolly A., Lemaire J.L., Belle-Oudry D., et al., 1997, J. Phys. B: At Mol Opt Phys 30, 4315
Jolly A., McPhate J.B., Lecavelier A., et al., 1998, A&A 329, 1028
Jordan C., Bartoe J.D.F., Bruecjner G.E., et al., 1979, MNRAS 187, 473
Kanik I., James G.K., Ajello J.M., 1995, Phys. Rev. A 51, 2067
Kirby K., Cooper D.L., 1989, J. Chem. Phys. 90, 4895
Krupenie P.H., 1966, Nat. Std. Ref. Data Ser., Nat. Bur. Std. (U.S.) 5
Lambert D.L., Sheffer Y., Gilliland R.L., Federman S.R., 1994, ApJ 420, 756
Lassettre E.N., Skerbele A., 1971, J. Chem. Phys. 54, 1597
LeFloch A., 1991, Mol. Phys. 72, 133
Letzelter C., Eidelsberg M., Rostas F., Breton J., Thieblemont B., 1987, Chem. Phys. 11,4 273
Liu X., Ahmed S.M., Multari R., James G.K., Ajello J.M., 1995, ApJS 101,375
Lyu C., Smith A.M., Bruhweiler F.C., 1994, ApJ 426, 254
Morton D.C., Noreau L., 1994, ApJS 95, 301
Mumma M.J., Morgan, H.D., Mentall J.E., 1975, J. Geophy. Res. 80,168
Mumma M.J., Stone E.J., Zipf E.C., 1971, J. Chem. Phys. 54, 2627
Raymond J.C., Blair W.P., Long K.S., 1997, ApJ 489, 314
Sheffer Y., Federman S.R., Lambert D.L., Cardelli J.A., 1992, ApJ 397, 482
Shemansky D.E., Ajello J.M., Kanik I., 1995, ApJ 452, 472

Smith P.L., Stark G., Yoshino K., Ito K., 1994, ApJ 431, L413
Spielfiedel A., Tchang-Brillet W.U.L., Dayou F., Feautrier N., 1998, A&A (in press)
Stark G., Lewis B.R., Gibson S.T., England J.P., 1998, ApJ (in press)
Telle H., Telle U., 1982, Comp. Phys. Comm. 28, 1
Tilford S.G., Simmons J.D., 1972, Phys. Chem. Ref. Data 2, 147
Wells W.C., Isler R.C., 1970, Phys. Rev. Letters 24, 705
Zetner P.W., Kanik, I. And Trajmar, S., 1998, J. Phys. B: At. Mol. Opt. Phys. 31, 2395
Zhong Z.P., Feng R.F., Xu K.Z., et al., 1997, Phys. Rev. A 55, 1997